

Release of Quantum Dot Nanoparticles in Porous Media: Role of Cation Exchange and Aging Time

Saeed Torkzaban,^{†,*} Scott A. Bradford,[‡] Jiamin Wan,[§] Tetsu Tokunaga,[§] and Arash Masoudih^{||}

[†]CSIRO, Land and Water, Glen Osmond, SA 5064, Australia

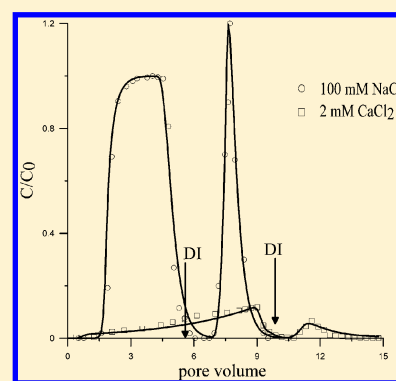
[‡]USDA, ARS, U.S. Salinity Laboratory, Riverside, California 92507, United States

[§]Lawrence Berkeley National Laboratory, 1 Cyclotron Road, Berkeley, California 94720, United States

^{||}Civil Engineering, The Catholic University, Washington, DC 20064, United States

S Supporting Information

ABSTRACT: Understanding the fate and transport of engineered nanoparticles (ENPs) in subsurface environments is required for developing the best strategy for waste management and disposal of these materials. In this study, the deposition and release of quantum dot (QD) nanoparticles were studied in saturated sand columns. The QDs were first deposited in columns using 100 mM NaCl or 2 mM CaCl₂ solutions. Deposited QDs were then contacted with deionized (DI) water and/or varying Na⁺ concentrations to induce release. QDs deposited in 100 mM Na⁺ were easily reversible when the column was rinsed with DI water. Conversely, QDs deposited in the presence of Ca²⁺ exhibited resistance to release with DI water. However, significant release occurred when the columns were flushed with NaCl solutions. This release behavior was explained by cation exchange (Ca²⁺ in exchange sites were replaced by Na⁺) which resulted in the breakdown of calcium bridging. We also studied the effect of aging time on the QD release. As the aging time increased, smaller amounts of QDs were released following cation exchange. However, deposited QDs were subsequently released when the column was flushed with DI water. The release behavior was modeled using a single first-order kinetic release process and changes in the maximum solid phase concentration of deposited QDs with transition in solution chemistry. The results of this study demonstrate that the presence of carboxyl groups on ENPs and divalent ions in the solution plays a key role in controlling ENP mobility in the subsurface environment.



INTRODUCTION

The increasing use of nanotechnology in a wide range of applications and products will inevitably result in the dissemination of engineered nanoparticles (ENPs) into the environment.¹ ENPs can partition to and from solid surfaces during subsurface transport. The process of ENP attachment or deposition from the solution to the solid surface has been extensively examined in a number of laboratory investigations.^{2–9} In contrast, the reverse process of detachment or release of deposited ENPs from the solid surface to solution has received much less attention.^{7,10,11} The release of deposited ENPs is an important step to initiate migration, and a comprehensive understanding of this process is therefore needed to predict ENP transport and fate in subsurface environments and for developing the best strategy for waste management and disposal of these materials.

The release of deposited ENPs is expected to be controlled by the hydrodynamics of the flow field, diffusion, and the strength of interactions between the particles and solid surface.^{12–17} However, it has been noted that the influence of hydrodynamics forces on particle release is typically negligible for submicrometer particles.^{18,19} Furthermore, laboratory column studies have demonstrated that the diffusion-controlled

release rate of ENPs is very small during steady-state flow and chemistry conditions.^{6,10} Conversely, rapid particle release has been observed during transient chemical conditions due to changes in ENP-solid interaction energies.^{12,15} Derjaguin, Landau, Verwey, and Overbeek (DLVO) theory^{20,21} is commonly employed to determine the interaction energy and/or force between colloids and solid surfaces for different solution chemistry conditions. DLVO theory considers interactions arising from electrostatics and van der Waals forces, but may be extended (XDLVO) to account for other interactions arising from Born repulsion, steric interactions, hydrophobic interactions, and/or hydration forces.^{21,22}

It is relatively easy to release ENPs that are deposited in the presence of monovalent ions by rinsing the porous medium with a low ionic strength (IS) solution.^{10,11} This release was attributed to a reduction in the depth of the secondary energy minimum.³ Secondary energy minima of the DLVO energy profile are small for nanosized particles in natural waters under

Received: May 9, 2013

Revised: August 21, 2013

Accepted: September 16, 2013

Published: September 16, 2013

typical IS conditions, and they may be eliminated by reducing the IS.¹⁹ In contrast to monovalent ions, ENPs deposited in the presence of divalent cations (such as Ca^{2+}) are reported to be highly resistant to release with a decrease in IS.^{10,11,15,23} These findings have been generally attributed to deposition in a primary minimum because it was assumed that no energy barrier existed in the presence of Ca^{2+} and a large energy barrier was created after lowering the IS.¹⁰

Cation exchange has also been demonstrated to have an important influence on microsized particle release.^{15,24–26} In particular, deposited particles can be released when divalent cations on the exchanger phase are replaced by monovalent cations.^{25,27} However, our understanding on the influence of cation exchange on particle release is still incomplete, especially for ENPs.¹⁵ For example, particle release sometimes does not occur with cation exchange, but rather depends on the combination of cation exchange followed by IS reduction.²⁴ In addition, in some cases an aging effect has been shown to be important in the kinetics of particle release.^{26,28} The likelihood of particle release became smaller the longer the particle was attached to the surface.²⁶ Furthermore, the release behavior is expected to depend on the nature of ENP-solid interaction. Surface modified ENPs have been demonstrated to interact with divalent ions by cation bridging which is not considered in classical DLVO calculations.²⁹ The influence of surface charge heterogeneity (such as adsorbed multivalent cations) on interaction energies is also known to be a function of the particle size, with smaller particles experiencing strong interactions.^{30,31} To the best of our knowledge, the effects of cation exchange and aging time on the release behavior of ENPs have not yet been systematically examined.

A number of modeling efforts has examined microsized particle release in porous media with reductions in solution IS,^{17,32–36} whereas relatively few modeling studies have considered the influence of cation exchange.³⁶ The mobilization of colloids has usually been modeled as a first-order kinetic attachment and detachment process in which parameters values are empirical functions of the solution chemistry. However, there is abundant experimental evidence indicating that the release of particles is a highly nonexponential process which is inconsistent with first-order kinetics.^{27,36} To account for such deviations, multiple attachment and/or detachment sites have been employed in models to account for the effects of heterogeneity in the particle population on release.^{34–36} Alternatively, particle release can be modeled using a single detachment coefficient and changes in the fraction of the surface area that contributes to particle immobilization and release with transients in solution chemistry.¹⁷ Systematic modeling studies on ENP release with transients in cation exchange, IS, and aging time have not yet been reported.

Quantum dots (QD) are one example of ENPs with diameters in the 2–100 nm size range that may be used for applications such as solar energy conversion, medical diagnostics, drug delivery, and light-emitting diodes.³⁷ QDs consist of a metalloid crystalline core (e.g., CdTe, CdSe) and often a protective shell (e.g., ZnS, CdS). The nanoparticles can then be made water-soluble by encapsulation in hydrophilic polymers containing carboxylic acid groups.³⁸ In this study, we examined and modeled the release behavior of QDs as a representative for surface-modified ENPs. A series of saturated packed-column experiments was conducted with the QDs suspended in two types of background electrolyte solutions (100 mM NaCl and 2 mM CaCl_2) buffered at pH 8. Deposited

QDs were subsequently contacted with different electrolyte solutions such as deionized (DI) water and varying Na^+ electrolyte concentrations to induce release via expansion of the double layer thickness and cation exchange, respectively. In addition, we studied the effect of aging time (i.e., the time that deposited QDs were allowed to stay on the solid surface in the presence of Ca^{2+} before altering the solution chemistry) on the QD release. A calibrated model provided a satisfactory description of the observed release behavior, and parameter values gave valuable insight on mechanisms of particle release.

■ MATERIAL AND METHODS

Preparation and Characterization of the Nanoparticles. Water-soluble poly(acrylic acid) capped CdTe QDs with diameters between 1 and 10 nm were supplied from Vive Nano Inc., Canada. Analytical reagent-grade NaCl and CaCl_2 (Fisher Scientific) and DI water were used to prepare electrolyte solutions of varying concentration (2 mM Ca^{2+} and 1–100 mM Na^+) buffered at pH 8 with 0.1 mM NaHCO_3 (Fisher Scientific). The QD stock with a CdTe suspension concentration of 18 mM (determined by ICP-MS) was diluted by a factor of 1000 in the various electrolyte solutions. The QD concentration in the electrolyte solutions was estimated to be about 2×10^{10} particles per ml based on the QD aggregate size of 90 nm and the CdTe density of 5.85 g/cm³.

Zeta potentials of the QDs in 100 mM NaCl and 2 mM CaCl_2 solutions were measured to be about -30 mV.²⁹ Zeta potentials of the silica sand in 100 mM NaCl and 2 mM CaCl_2 solutions were estimated to be -15 and -30 mV, respectively.³⁹ The average aggregate diameters of QDs in 100 mM NaCl and 2 mM CaCl_2 solutions assessed using dynamic light scattering were stable over the time span of 350 min and were about 55 and 90 nm, respectively.²⁹ Different aggregation diameters could be attributed to the nonuniform coating of QD particles with poly(acrylic acid) ligands, and the surrounding electrical double layer.²⁹ We, therefore, concluded that the effect of QD aggregation in the transport experiments was minimal for our solution chemistry conditions.

Porous Media. Sand from Unimin Corporation (Le Sueur, MN) was used as the porous media for transport experiments. The average grain diameter of the sand was 270 μm , and the grain size ranged from 250 to 300 μm . The following cleaning protocol was employed to clean and remove impurities from the sand. The sand was soaked in 70% HNO_3 for 16 h and rinsed with DI water until the pH was equilibrated.²⁹ The sand was then immersed in 0.5 M NaCl solution for 1 h in a sonication bath, rinsed with DI water, and then sonicate in DI water for 1 h. These steps (i.e., soaking in 0.5 M NaCl solution, rinsing with DI water, and sonication) were repeated three times. Scanning electron microscopy (Zeiss Gemini, Ultra-55) images demonstrated that the surfaces of the sand grains were largely emptied of the clay particles by this cleaning treatment.

Deposition and Release Experiments. Experiments were conducted using a 10 cm acrylic column with a 2.5 cm inner diameter. The columns were wet-packed and the porosity was determined to be about 0.41 from analysis of the breakthrough concentrations (BTCs) of a conservative tracer (NaNO_3). Different electrolyte solutions discussed below were flushed through the vertically oriented columns at a constant average pore-water velocity of 7 m/day using a syringe pump. This value of water velocity was selected to represent a typical water velocity found in coarse textured porous media. The columns were flushed with 5 pore volumes (PVs) of electrolyte solution

of interest before initiating the experiments. One PV corresponds to a column residence time of 20.5 min.

QDs suspended in either 100 mM Na⁺ (~ 4 PVs) or 2 mM Ca²⁺ (~9 PVs) were introduced into the columns during phase 1 (deposition phase), followed by elution with QD-free electrolyte solution as used during phase 1 (phase 2). Different pulse durations of QDs were applied for the injection of QDs in Na⁺ and Ca²⁺ electrolytes in order to investigate their deposition behavior on the sand surfaces. Systematic studies on the deposition behavior of QDs in the presence of monovalent and divalent cations over a wide range of solution IS have been reported elsewhere.^{6,29} Phase 3 consisted of flushing a few PVs of DI water buffered to pH 8 (with 0.1 mM NaHCO₃) into the column in an effort to release the deposited QDs.

A set of experiments was conducted to examine the influence of cation exchange on the release of deposited QDs. The QD deposition in these experiments was conducted using 2 mM CaCl₂ as the background electrolyte. Following phase 3 in which the column was flushed with DI water at pH 8, several pore volumes of NaCl solutions with various concentrations (20, 30, 50, and 100 mM) was introduced into the column (phase 4). In an effort to understand the effect of aging on the release behavior of the QDs, a similar series of deposition (in the presence of 2 mM Ca²⁺) and cation exchange release experiments were conducted in which the flow was halted (i.e., no flow conditions) for about 16 and 48 h at the end of phase 2. Following the flow interruption, the flow was resumed by eluting the column with DI water (phase 3), cation exchange phase (phase 4), and finally another round of flush with DI water buffered at pH 8 (phase 5). The pulse duration of each phase in the column experiments in terms of the number of pore volumes is provided in Supporting Information (SI) Table S1.

Column effluent during the experiments was collected using a fraction collector and analyzed for the QD concentration by either UV/vis spectrometer or ICP-MS (Perkin-Elmer DRC II) by measuring the Cd concentration of the samples. The concentration of calcium in some of the effluent samples was measured with the ICP-MS. It is worthwhile to mention that most of the transport experiments presented in this work were conducted at least in duplicate and exhibited good reproducibility.

Mathematical Model. The transport, deposition, and release of the QDs in the packed column experiments were simulated using the one-dimensional form of the advection–dispersion equation (ADE) that includes first-order kinetic terms for attachment and detachment. The aqueous and solid phase mass balance equations for QDs during phases 1 and 2 are given as follows:

$$\frac{\partial(\theta C)}{\partial t} = -\frac{\partial J}{\partial z} - \theta \psi k_{\text{dep}} C \quad (1)$$

$$\frac{\partial(\rho_b S)}{\partial t} = \theta \psi k_{\text{dep}} C \quad (2)$$

where θ [–] is the volumetric water content, t [T; T denotes units of time] is time, and z [L; L denotes units of length] is the depth, ρ_b [M L³; where M is the units of mass of sand] is the solid phase bulk density, C [M_{cd} L^{−3}; M_{cd} denotes the cadmium concentration] is the concentration of QDs in the aqueous phase, J [M_{cd} L^{−2} T^{−1}] is the flux (sum of the advection and dispersion flux) of QDs, S [M_{cd} M^{−1}] is the concentration of

QDs on the solid phase, and k_{dep} [T^{−1}] is the QD deposition rate coefficient from the aqueous to the solid phase. The parameter ψ [–] accounts for time and concentration dependent blocking using a Langmuirian approach as

$$\psi = 1 - \frac{S}{S_{\text{max}}} \quad (3)$$

where S_{max} [M_{cd} M^{−1}] is the maximum solid phase concentration of deposited QDs.

QD detachment was not considered during phases 1 and 2 because tailing of the BTCs was negligible under steady-state chemical conditions. In contrast, significant amounts of QDs were released during phases 3–5 with transients in solution chemistry. In this case, the release process needs to be coupled with the solution chemistry. Chemical changes (e.g., IS, pH, and cation exchange) take place within chromatographic fronts traveling through the porous medium.³⁶ In natural soils with substantial clay contents, the resulting travel velocities of these fronts are retarded in comparison to that of a conservative tracer. However, the travel velocity of a chromatographic front approaches that of a conservative tracer in sands with a very low cation exchange capacity (CEC) under equilibrium conditions. The treated sand employed in this study contained a negligible amount of clay, and a very low CEC. An initial approximation of the chromatographic front for Ca²⁺ and Na⁺ in this study was therefore determined from the solution of the mass balance equation for a conservative tracer.

$$\frac{\partial(\theta C_s)}{\partial t} = -\frac{\partial J_s}{\partial z} \quad (4)$$

where C_s [M_s L^{−3}; M_s denotes the mass] is the ion concentration in the aqueous phase, and J_s [M_s L^{−2} T^{−1}] is the ion flux (sum of the advection and dispersion flux). The transport and release of QDs during phase 3, 4, and 5 was subsequently simulated as

$$\frac{\partial(\theta C)}{\partial t} = -\frac{\partial J}{\partial z} + \rho_b k_{\text{rel}} (S - f_{\text{nr}} S_i) \quad (5)$$

$$\frac{\partial(\rho_b S)}{\partial t} = -\rho_b k_{\text{rel}} (S - f_{\text{nr}} S_i) \quad (6)$$

where S_i [M_{cd} M^{−1}] is the value of S at the end of the phase 2 and before a change in solution chemistry (e.g., ion type), f_{nr} [–] is the fraction of deposited QDs that are not released upon a change in chemical composition (i.e., DI water or cation exchange), and k_{rel} [T^{−1}] is the QD release rate coefficient from the solid phase to the aqueous phase. The parameters f_{nr} and k_{rel} are functions of C_s that will be described below. QD redeposition was considered to be negligible during the release phase because it was assumed that the conditions were unfavorable for deposition.

The fraction of QDs released with transients in solution chemistry, $f_r = (1 - f_{\text{nr}})$, is directly related to changes in the balance of resisting adhesive torque and the applied hydrodynamic torque.^{40,41} Bradford et al.¹⁷ demonstrated that the value of f_{nr} can be determined as

$$f_{\text{nr}} = \frac{S_{\text{max}}}{S_{\text{imax}}} = \frac{S_{\text{eq}}}{S_i} \quad (7)$$

where S_{imax} [M_{cd} M^{−1}] is the value of S_{max} during phases 1 and 2, and S_{eq} [M_{cd} M^{−1}] is the equilibrium value of S at the end of the chemical perturbation. The value of S_{eq} was determined by

conducting a mass balance calculation for each step in chemical perturbation (release phases 3–5), and f_{nr} and S_{max} were calculated from this information using eq 7. Consequently, f_{nr} can be determined by fitting the obtained BTCs during release phases 3–5 to the solution of the outlined equations. Alternatively, values of f_{nr} can be estimated from the fraction of the solid surface area that contributes to colloid immobilization by conducting a balance of applied hydrodynamic and resisting adhesive torques over the surface of the porous medium.⁴¹

The value of k_{rel} is controlled by interactions between the QDs and the solid surface that change with solution chemistry. This should theoretically be a very rapid response, as has been confirmed in literature.^{17,34} The value of k_{rel} was determined as¹⁷

$$k_{rel} = k_{sw}H_0(S - f_{nr}S_i)H_0(C_s - 0.5C_{si}) \quad (8)$$

where k_{sw} [T^{-1}] is the mass transfer coefficient from the solid to the bulk aqueous phase, $H_0(S - f_{nr}S_i)$ is the Heaviside function that is equal to 1 when $S > f_{nr}S_i$ and 0 when $S \leq f_{nr}S_i$ and $H_0(C_s - 0.5C_{si})$ is the Heaviside function that is equal to 1 when $C_s > 0.5C_{si}$ and 0 when $C_s \leq 0.5C_{si}$; C_{si} is the input Na^+ concentration.

The code developed by Massoudieh and Ginn⁴² was used to model the one-dimensional transport of conservative ions (Na^+) and QDs. The parameters were estimated using a hybrid genetic algorithm⁴³ and simplex optimization.^{44,45} The parameters k_{dep} and S_{max} were determined by optimization to BTCs of QDs during phases 1 and 2. Values of k_{sw} were obtained by optimization to the QD release data during DI water and Na^+ injection phases (phases 3–5). The dispersivity λ was estimated to be 0.1 cm based on the results of tracer data. All simulations employed a third type boundary condition (e.g., a time dependent colloid flux) at the column inlet to ensure conservation of mass at the boundary. The dispersive flux was set to zero at the column outlet.

RESULTS AND DISCUSSION

QD Deposition and Release with DI water. Figure 1 shows observed and simulated BTCs of the QDs during phases 1–3 when the QDs during phase 1 (deposition phase) were suspended in 100 mM Na^+ or 2 mM Ca^{2+} solutions. In this figure and elsewhere the effluent concentrations (C) are normalized by the input concentration (C_0) and plotted versus the number of PVs passed through the column. To quantitatively compare the experiments, the BTCs of phases 1 and 2 were simulated with eqs 1–3 using fitted values of k_{dep} and S_{max}/C_0 which are given in SI Table S1. The release behavior during phases 3–5 was subsequently simulated with eqs 4–8 using fitted values of k_{sw} and calculated values of S_{max}/C_0 (eq 7). Parameter values (k_{sw} , f_{nr} , and S_{max}/C_0) of the release phases are given in Table 1, along with the coefficient of linear regression (R^2). It is observed that the deposition, blocking, and release model accurately described the BTCs and release behavior of QDs during phases 1–3 ($R^2 > 0.95$).

QDs suspended in 100 mM Na^+ reached the influent concentration after about 2 PVs during phase 1. In a remarkable contrast, QDs suspended in 2 mM Ca^{2+} only reached a peak value of $C/C_0 = 0.06$ after 9 PVs during phase 1 and ~94% of the injected QDs were deposited in the sand. In an attempt to explain these observations, the DLVO energy profiles for the QDs and sand were calculated (SI Figure S1). Because our QDs

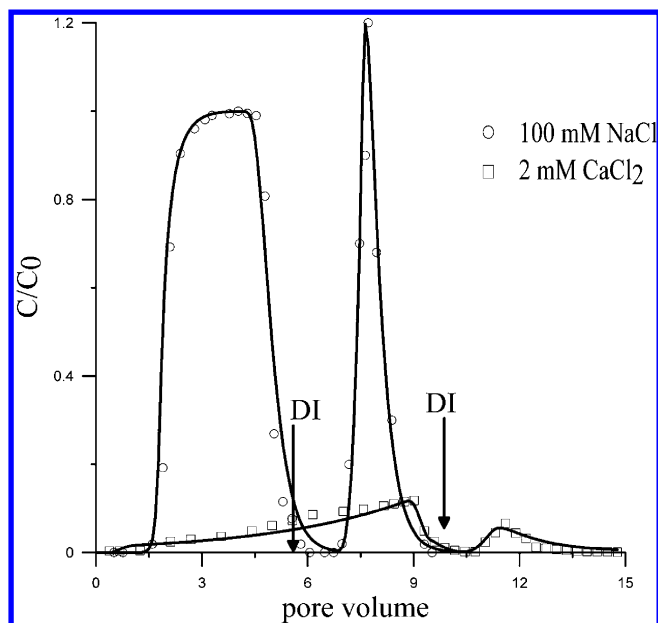


Figure 1. Observed effluent concentration and corresponding model fits for representative effluent concentrations of QDs for experiments conducted in the presence of 100 mM Na^+ and 2 mM Ca^{2+} . QDs deposited in the presence of Na^+ were easily released (~100%) by rinsing the column with DI water. When QDs were deposited in the presence of Ca^{2+} , very small amount of release occurred by rinsing the column with DI water.

Table 1. Calculated and Fitted Model Parameters for the Release Experiments

release solution	deposition solution	k_{sw}^a min ⁻¹	$f_r = (1 - f_{nr})^b$	S_{max}/C_0^b cm ³ g ⁻¹	R^2 %
DI Water (Phase 3)					
	100 mM NaCl	0.27 ± 0.02	0.99	0.035	98
	2 mM CaCl ₂	0.036 ± 0.005	0.014	3.47	98
Phase 4					
20 mM NaCl	2 mM CaCl ₂	0.026 ± 0.06	0.83	0.59	97
30 mM NaCl		0.03 ± 0.004	0.95	0.17	98
50 mM NaCl		0.07 ± 0.002	0.8	0.70	97
100 mM NaCl		0.10 ± 0.03	0.75	0.88	96

^aDetermined by fitting the obtained BTCs during the release phases to the solution of eqs 1–8. ^bDetermined from a mass balance calculation of the BTCs and using eq 7.

were functionalized with poly(acrylic acid), we assumed a value of 4.04×10^{-21} J for the Hamaker constant which is consistent with the reported value for carboxylate-modified polystyrene latex particles.⁴⁶ DLVO calculations predicted the presence of a repulsive energy barrier of ~12 kT and a shallow secondary energy minimum between QDs and sand in 100 mM $NaCl$. A very small amount of QD deposition in the presence of 100 mM Na^+ may occur due to the presence of this shallow secondary minimum and/or nanoscale heterogeneity on the sand surface.⁶ DLVO calculations suggested an even higher energy barrier against deposition in the presence of 2 mM Ca^{2+} (SI Figure S1). Conversely, the BTC data (Figure 1) showed significant deposition in the presence of Ca^{2+} . It is evident that the observed deposition behavior for QDs in the presence of 2 mM Ca^{2+} cannot be explained by standard DLVO calculations

on homogeneous surfaces. However, attachment of the negatively charged QDs on negatively charged sand surfaces can be explained by the formation of divalent cation (Ca^{2+}) bridging as previously described by Torkzaban et al.²⁹ Such ion–ion correlation forces cannot be explained on the basis of the Poisson–Boltzmann model on homogeneous surfaces.^{47,48} However, Bradford and Torkzaban^{30,31} demonstrated that localized chemical and physical heterogeneities on the colloid and/or mineral solid surfaces may enhance particle attachment under unfavorable (repulsive) attachment conditions. These results qualitatively demonstrate the effects of chemical heterogeneities in which complexation of Ca^{2+} ions to the silanol groups on the mineral surfaces and carboxylic acid groups on the surface of QDs produced localized favorable sites for deposition.

Values of k_{dep} were higher when the solution contained 100 mM Na^+ (3.1 min^{-1}) than 2 mM Ca^{2+} (0.18 min^{-1}). Conversely, the fitted values of S_{max}/C_0 were much lower in the presence of 100 mM Na^+ ($0.2 \text{ cm}^3 \text{ g}^{-1}$) than in the presence of 2 mM Ca^{2+} ($3.47 \text{ cm}^3 \text{ g}^{-1}$). The causes for these differences in k_{dep} and S_{max}/C_0 were discussed in detail in our previous publications.^{6,29} In brief, the higher value of k_{dep} in the presence of 100 mM Na^+ was likely due to a deeper secondary energy minimum in 100 mM Na^+ than in 2 mM Ca^{2+} resulting in higher solid phase migration of particles.⁴⁹ The larger value of S_{max}/C_0 in the presence of 2 mM Ca^{2+} was due to larger localized favorable sites, produced by cation bridging, for deposition. Very few QDs were released during phase 2 (negligible tailing) when the columns were flushed with either 100 mM Na^+ or 2 mM Ca^{2+} solutions. We, therefore, considered a zero detachment rate coefficient during phases 1 and 2. However, when DI water was flushed through the column containing QDs deposited in 100 mM Na^+ solution, a large peak of QDs occurred during phase 3. Calculations of QD mass balance in the column effluent revealed that more than 99% of the deposited QDs were eluted with the DI water. Furthermore, the value of k_{sw} was very high (0.27 min^{-1}), indicating that the release occurred rapidly and was not diffusion controlled. Similarly, S_{max}/C_0 significantly decreased by about 1 order of magnitude from $0.2 \text{ cm}^3 \text{ g}^{-1}$ (phases 1 and 2) to $0.035 \text{ cm}^3 \text{ g}^{-1}$ (phase 3) with a reduction in IS.

Figure 1 shows that only a very small amount of the QDs deposited in the presence of 2 mM Ca^{2+} (phase 1) were released upon introduction of DI water (phase 3). The value of k_{sw} was therefore very low (0.036 min^{-1}) and S_{max}/C_0 did not change much ($3.52\text{--}3.47 \text{ cm}^3 \text{ g}^{-1}$). It has been reported that microsized particles that are deposited in the presence of divalent ions (e.g., Ca^{2+}) are resistant to release upon a reduction in the solution IS.^{24,50} This resistance to release at low IS is consistent with cation bridging complexation being the underlying mechanism for deposition. The small release of microsized particles has been explained by the selectivity of most natural mineral surfaces for divalent over monovalent cations.²⁵ Removal of divalent ions from the exchanger phase of charged colloidal particles and mineral surfaces occurs very gradually with a reduction in solution IS.^{25,51} Consequently, we believe that the strength of the QD–sand interaction arising from cation bridging was not much influenced by a reduction in solution IS to DI water, and therefore resulted in little QD release.

QD Release Induced by Cation Exchange. A series of release experiments was conducted in which the QDs suspended in 2 mM Ca^{2+} were eluted with DI water (phase

3) and then flushed with varying concentrations of Na^+ electrolytes (20, 30, 50, and 100 mM NaCl solutions). Figure 2 presents representative observed and simulated BTCs for

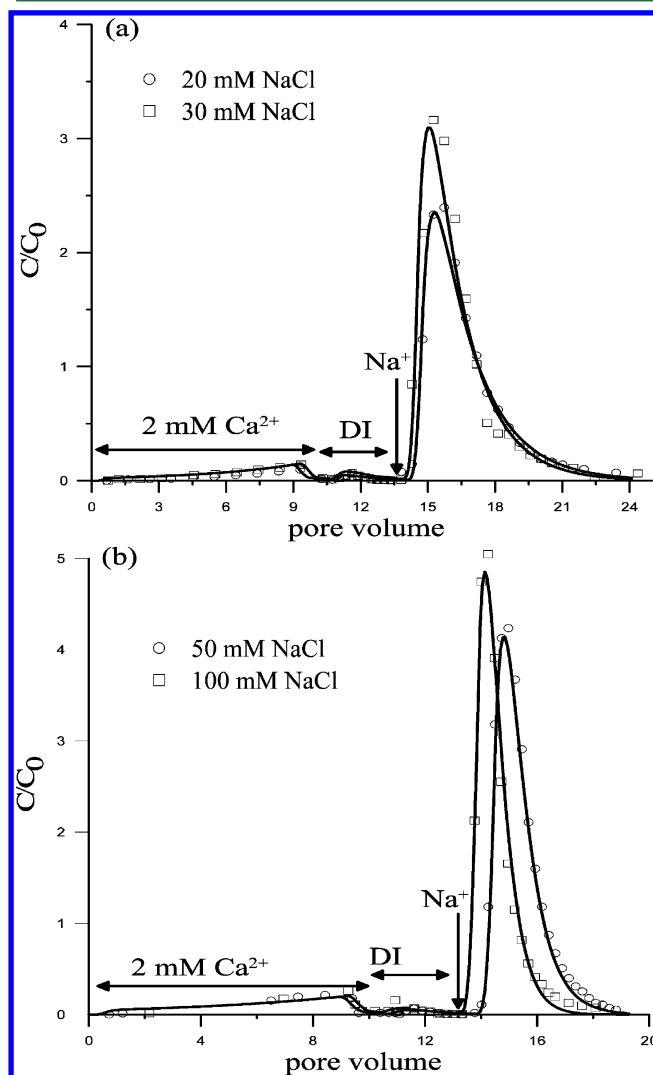


Figure 2. Observed effluent concentration and corresponding model fits for release of QDs deposited in the presence of 2 mM Ca^{2+} (~ 9 PV injection) after the columns were flushed with DI water followed by various concentrations of NaCl electrolytes: (a) 20 and 30 mM NaCl , (b) 50 and 100 mM NaCl .

QDs during phases 1–4 as a function of PVs. Similar to Figure 1, very little QD release occurred with DI water during phase 3 in all experiments. In contrast, a substantial amount of deposited QDs were released when the column was flushed with NaCl electrolyte during phase 4. The mass balance calculations revealed that the maximum release occurred with 30 mM NaCl solution (95%) and decreased with further increase of Na^+ concentrations (Table 1). However, the peak concentration of the BTCs increased with the Na^+ concentration, indicating that the release rate increased with the Na^+ concentration.

Table 1 provides a summary of fitted (k_{sw}) and calculated (S_{max}/C_0) model parameters. The optimized model provided an excellent description of the QD release. Higher values of k_{sw} were required to accurately capture the observed release behavior with increasing Na^+ concentration. High values of k_{sw}

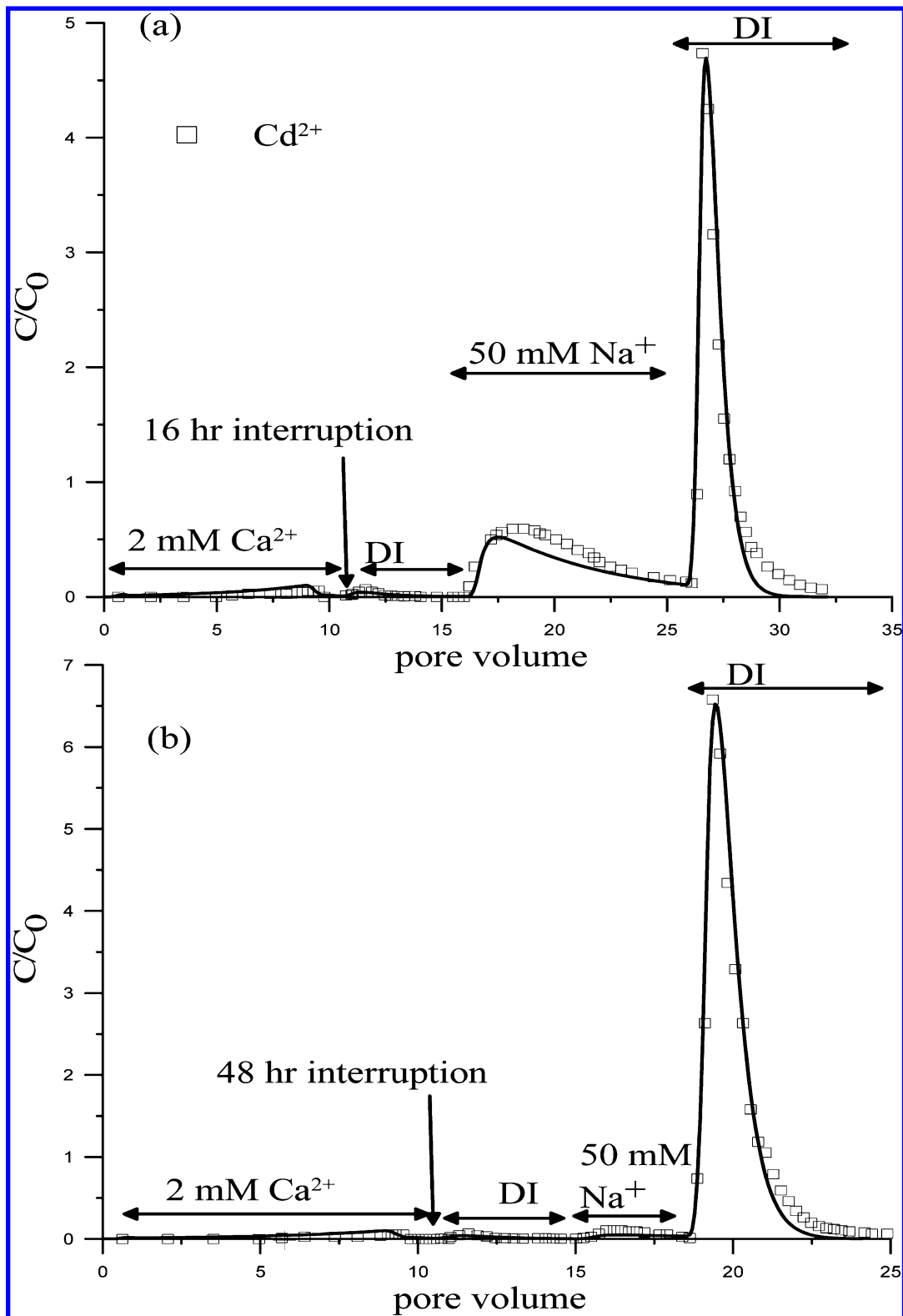


Figure 3. Observed effluent concentration and corresponding model fits showing the effect of flow interruption on QD release: (a) 16 h flow interruption; (b) 48 h flow interruption. Compare these observations with those of Figure 2b (50 mM NaCl, no flow interruption). Note that the longer the deposited QDs were in the presence of Ca^{2+} , the less release occurred upon introduction of NaCl electrolyte. A complete recovery of deposited QDs was obtained after the injection of DI water at the end of the experiments.

are not consistent with a slow diffusion-controlled process as is commonly assumed,⁵² but are rather controlled by system hydrodynamics and changes in the torque and force balances with transients in solution chemistry.⁵³ Cation exchange

provides a partial explanation for the observed release behavior of the QDs during phase 4. It has been demonstrated that when mineral surfaces exhibit a selectivity for a particular cation, the exchange of that cation for a lower selectivity cation will occur

only when the less selective ion is present at high concentrations.^{25,51} To confirm the occurrence of cation exchange of Ca^{2+} for Na^+ , SI Figure S2 presents the effluent concentrations of QDs and Ca^{2+} in the cation exchange release experiment during phases 3 (DI water) and 4 (50 mM NaCl). The adsorbed Ca^{2+} on the sand surface was not released with DI water during phase 3. However, a simultaneous release of QDs and Ca^{2+} occurred when the column was flushed with 50 mM NaCl as a result of cation exchange.

The effect of cation exchange on the QD release process shown in Figure 2 can therefore be explained as follows. When DI water was introduced to the column where QDs were in equilibrium with 2 mM Ca^{2+} , a negligible amount of Ca^{2+} enters the aqueous phase from the solid phase and very low amounts of QDs were released. However, when a solution with Na^+ was injected into a column during phase 4, Ca^{2+} was removed from the exchanger phase to a greater extent by Na^+ than with DI water. This cation exchange sequence (Na^+ for Ca^{2+}) reduces the amount of cation bridging, and thereby promotes QD release. Higher peak concentrations of QDs occurred with increasing Na^+ due to greater amounts of cation exchange. However, mass balance calculations showed that the greatest total amount of release occurred at 30 mM Na^+ concentration (95%), and that further increase of the NaCl concentration (i.e., 50 and 100 mM) resulted in a decrease in the amount of QD release. These observations may be explained by the fact that when the Ca^{2+} was replaced by Na^+ , increases in the Na^+ concentration with higher IS may cause more QDs to deposit in a deeper secondary minimum or nanoscale chemical heterogeneities.⁶ Values of S_{max} depend on both the amount of cation bridging and secondary minimum interactions, and consequently follow similar trends to the overall mass balance. Indeed, it was observed that when the column was finally flushed with DI water during phase 5, removing the Na^+ from the sand surface by DI water, the remaining deposited QDs were released and a mass balance ranging from 96 to 105% was achieved.

Aging Effect. Additional experiments were conducted to understand the effect of aging time on the release behavior of QDs initially deposited in 2 mM Ca^{2+} solution. To this end, the flow was halted for about 16 and 48 h after completion of phase 2 before initiating the release with DI water (phase 3), 50 mM Na^+ (phase 4), and DI water (phase 5). Observed and simulated results from these flow interruption experiments are shown in Figure 3. The simulations provided a good description of the QD release for the various aging times. Table 2 provides a summary of fitted values of k_{sw} and calculated values of S_{max}/C_0 for these aging experiments.

In dramatic contrast to the uninterrupted flow experiments shown in Figure 2, very small amounts of QDs were released in the aging experiments with 50 mM Na^+ solution during phase 4. As the flow interruption time increased, a smaller amount of QDs was released following the cation exchange process (phase 4). Increasing the aging time to 48 h did not influence k_{sw} or S_{max}/C_0 in the presence of DI water (phase 3), but produced about 7-fold decrease in k_{sw} and a greater than 4 fold increase in S_{max}/C_0 in the presence of 50 mM Na^+ (phase 4). These observations indicate that the QD deposition aging time had a significant effect on their subsequent release. For example, when the deposited QDs were left on the sand surface for about 48 h, elution with 50 mM Na^+ caused release of only around 5%. In contrast, 80% of the deposited QDs were recovered with 50 mM Na^+ when the flow was uninterrupted (aging time of 0).

Table 2. Calculated and Fitted Model Parameters for the Aging Experiments

release solution	interruption time	$k_{\text{sw}}^a \text{ min}^{-1}$	$f_r = (1 - f_{\text{nr}})^b$	$S_{\text{max}}/C_0^b \text{ cm}^3 \text{ g}^{-1}$
DI water (phase 3)	0	0.037 ± 0.005	0.013	3.47
	16	0.035 ± 0.002	0.014	3.47
	48	0.034 ± 0.004	0.011	3.48
50 mM NaCl (phase 4)	0	0.07 ± 0.004	0.8	0.7
	16	0.0096 ± 0.001	0.4	2.1
	48	0.0095 ± 0.001	0.05	3.3
DI water (phase 5)	0	0.078 ± 0.003	1	0
	16	0.108 ± 0.005	1	0
	48	0.096 ± 0.002	1	0

^aDetermined by fitting the obtained BTCs during the release phases to the solution of eqs 1-8. ^bDetermined from a mass balance calculation of the BTCs and using eq 7.

It was observed that the remaining deposited QDs were subsequently released by flushing the column with DI water (phase 5), suggesting that release was dependent on both cation exchange and expansion of the double layer thickness.

These observations indicate that the strength of the QD-solid interaction increased with the deposition aging time. We postulate this occurred because greater numbers of calcium ions interacted with QDs during phase 2 as the aging time increased, and this influenced the kinetics and/or extent of binding between the QDs and mineral surface during phase 4. The amount and rate of cation exchange has been observed to change with the release of kaolinite particles.²⁴ The combination of cation exchange (phase 4) and expansion of the double layer thickness (phase 5) was therefore required to release the deposited QDs as the aging time increased.

ENVIRONMENTAL IMPLICATIONS

Most of the reported studies on surface-modified ENPs transport and deposition have been conducted using a monovalent ion as a background electrolyte.¹⁹ It is reported that surface-modified ENPs exhibit high stability and mobility in porous media raising concerns about potential adverse effects of these materials on the subsurface environment. However, our results suggest that deposition of surface-modified ENPs containing carboxylic groups may be profoundly enhanced in the presence of divalent ions due to formation of cation bridging. Moreover, it is expected that deposition of ENPs in the presence of divalent cations caused by cation bridging is resistant to release with a reduction to IS. However, the release may be induced when divalent cations in the bridging complexation are exchanged with monovalent ions. It was demonstrated that the strength of cation bridging interaction increased as the deposition time increased. This resulted in a small amount of release during the cation exchange process. Consequently, QD release was dependent on both cation exchange and expansion of the double layer thickness. Many natural environments experience changes in solution chemistry as a result of infiltration of different water qualities and compositions, evapotranspiration, mineral dissolution, groundwater recharge, and surface-groundwater interactions. Our results suggest that such transients in solution chemistry are likely to promote the episodic release and migration of ENPs in the subsurface environment.

■ ASSOCIATED CONTENT

■ Supporting Information

The following Supporting Information is available: The pulse duration of each phase in the column experiments and fitted values of k_{dep} and S_{max}/C_0 (Table S1); a brief description and discussion of the DLVO calculations and results (Figure S1); the effluent concentrations of QDs and Ca^{2+} in the cation exchange release experiment during phases 3 (DI water) and 4 (50 mM NaCl) (Figure S2). This material is available free of charge via the Internet at <http://pubs.acs.org>.

■ AUTHOR INFORMATION

Corresponding Author

*(S.T.) Phone: +61-8-8303 8491; e-mail: saeed.torkzaban@csiro.au

Notes

The authors declare no competing financial interest.

■ ACKNOWLEDGMENTS

Funding was provided through the joint BER-EPA-NSF Nanoparticulate Research Program of the Office of Biological and Environmental Research, U.S. Department of Energy, under contract DE-AC02-05CH11231.

■ REFERENCES

- (1) Klaine, S. J.; Alvarez, P. J. J.; Batley, G. E.; Fernandes, T. F.; Handy, R. D.; Lyon, D. Y.; Mahendra, S.; McLaughlin, M. J.; Lead, J. R. Nanomaterials in the environment: Behavior, fate, bioavailability, and effects. *Environ. Toxicol. Chem.* **2008**, *27* (9), 1825–1851.
- (2) Brant, J.; Lecoanet, H.; Wiesner, M. R. Aggregation and deposition characteristics of fullerene nanoparticles in aqueous systems. *J. Nanopart. Res.* **2005**, *7* (4–5), 545–553.
- (3) Li, Y.; Wang, Y.; Pennell, K. D.; Abriola, L. M. Investigation of the transport and deposition of Fullerene (C60) Nanoparticles in quartz sands under varying flow conditions. *Environ. Sci. Technol.* **2008**, *42*, 7174–7180.
- (4) Liu, X.; O'Carroll, D. M.; Petersen, E. J.; Qingguo, H.; Anderson, C. L. Mobility of multiwalled carbon nanotubes in porous media. *Environ. Sci. Technol.* **2009**, *43* (21), 8153–8158.
- (5) Phenrat, T.; Song, J. E.; Cisneros, C. M.; Schoenfelder, D. P.; Tilton, R. D.; Lowry, G. V. Estimating attachment of nano- and submicrometer-particles coated with organic macromolecules in porous media: Development of an empirical model. *Environ. Sci. Technol.* **2010**, *44* (12), 4531–4538.
- (6) Torkzaban, S.; Kim, Y.; Mulvihill, M.; Wan, J.; Tokunaga, T. Transport and deposition of functionalized CdTe nanoparticles in saturated porous media. *J. Contam. Hydrol.* **2010**, *118*, 208–217.
- (7) Quevedo, I. R.; Tufenkji, N. Influence of solution chemistry on the deposition and detachment kinetics of a CdTe quantum dot examined using a quartz crystal microbalance. *Environ. Sci. Technol.* **2009**, *43* (9), 3176–3182.
- (8) Quevedo, I. R.; Tufenkji, N. Mobility of functionalized quantum dots and a model polystyrene nanoparticle in saturated quartz sand and loamy sand. *Environ. Sci. Technol.* **2012**, *46* (8), 4449–4457.
- (9) Quevedo, I. R.; Olsson, A. L. J.; Tufenkji, N. Deposition kinetics of quantum dots and polystyrene latex nanoparticles onto alumina: Role of water chemistry and particle coating. *Environ. Sci. Technol.* **2013**, *47* (5), 2212–2220.
- (10) Jaisi, D. P.; Elimelech, M. Single-walled carbon nanotubes exhibit limited transport in soil columns. *Environ. Sci. Technol.* **2009**, *43* (24), 9161–9166.
- (11) Wang, Y.; Li, Y.; Pennell, K. D. Influence of electrolyte species and concentration on the aggregation and transport of fullerene nanoparticles in quartz sands. *Environ. Toxicol. Chem.* **2008**, *27*, 1860–1867.
- (12) Godinez, I. G.; Darnault, C. J.; Khodadoust, A. P.; Bogdan, D. Deposition and release kinetics of nano-TiO₂ in saturated porous media: Effects of solution ionic strength and surfactants. *Environ. Pollut.* **2013**, *174*, 106–113, DOI: 10.1016/j.envpol.2012.11.002.
- (13) Shen, C.; Li, B.; Wang, C.; Huang, Y.; Jin, Y. Surface roughness effect on deposition of nano- and micro-sized colloids in saturated columns at different solution ionic strengths. *Vadose Zone J.* **2011**, *10*, 1071–1081.
- (14) Shen, C.; Wang, F.; Li, B.; Jin, Y.; Wang, L.-P.; Huang, Y. Application of DLVO energy map to evaluate interactions between spherical colloids and rough surfaces. *Langmuir* **2012**, *28*, 14681–14692.
- (15) Shen, C.; Lazouskaya, V.; Jin, Y.; Li, B.; Zheng, W.; Ma, Z.; Huang, Y. Coupled factors influencing detachment of nano- and micro-sized particles from primary minima. *J. Contamin. Hydrol.* **2012**, *134–135*, 1–11.
- (16) Shen, C.; Li, B.; Huang, Y.; Jin, Y. Kinetics of coupled primary and secondary-minimum deposition of colloids under unfavorable chemical conditions. *Environ. Sci. Technol.* **2007**, *41*, 6976–6982.
- (17) Bradford, S. A.; Torkzaban, S.; Kim, H.; Simunek, J. Modeling colloid and microorganism transport and release with transients in solution ionic strength. *Water Resour. Res.* **2012**, *48*, 9 DOI: 10.1029/2012WR012468.
- (18) Khilar, K. C.; Fogler, H. S. *Migration of Fines in Porous Media*, Chapters 1 and 4; Kluwer Academic Publishers: Dordrecht, 1998.
- (19) Petosa, A. R.; Jaisi, D. P.; Quevedo, I. R.; Elimelech, M.; Tufenkji, N. Aggregation and deposition of engineered nanomaterials in aquatic environments: Role of physicochemical interactions. *Environ. Sci. Technol.* **2010**, *44*, 6532–6549.
- (20) Derjaguin, B. V.; Landau, L. D. Theory of the stability of strongly charged lyophobic sols and of the adhesion of strongly charged particles in solutions of electrolytes. *Acta Physicochim. URSS* **1941**, *14*, 733–762.
- (21) Verwey, E. J. W.; Overbeek, J. Th. G. *Theory of the Stability of Lyophobic Colloids*; Elsevier: Amsterdam, 1948.
- (22) Bradford, S. A.; Torkzaban, S. Colloid transport and retention in unsaturated porous media: A review of interface-, collector-, and pore scale processes and models. *Vadose Zone J.* **2008**, *7*, 667–681.
- (23) Chen, K. L.; Mylon, S. E.; Elimelech, M. Aggregation kinetics of alginate-coated hematite nanoparticles in monovalent and divalent electrolytes. *Environ. Sci. Technol.* **2006**, *40* (5), 1516–1523.
- (24) Bradford, S. A.; Kim, H. Implications of cation exchange on clay release and colloid-facilitated transport in porous media. *J. Environ. Qual.* **2010**, *39*, 2040–2046.
- (25) Roy, S. B.; Dzombak, D. A. Na⁺–Ca²⁺ exchange effects in the detachment of latex colloids deposited in glass bead porous media. *Colloids Surf., A* **1996a**, *107*, 223–231.
- (26) Grolimund, D.; Borkovec, M. Release of colloidal particles in natural porous media by monovalent and divalent cations. *J. Contam. Hydrol.* **2006**, *87*, 155–175.
- (27) Roy, S. B.; Dzombak, D. A. Colloid release and transport processes in natural and model porous media. *Colloids Surf., A* **1996b**, *107*, 245–262.
- (28) Kuo, R. J.; Matijevic, E. Particle adhesion and removal in model systems. Part 2. Monodispersed chromium hydroxide on steel. *J. Chem. Soc., Faraday Trans.* **1979**, *1* (75), 2014–2026.
- (29) Torkzaban, S.; Wan, J.; Tokunaga, T. K.; Bradford, S. A. Impacts of bridging complexation on the transport of surface-modified nanoparticles in saturated sand. *J. Contam. Hydrol.* **2012**, *136–137*, 86–95.
- (30) Bradford, S. A.; Torkzaban, S. Colloid adhesive parameters for chemically heterogeneous porous media. *Langmuir* **2012**, *28* (38), 13643–13651.
- (31) Bradford, S. A.; Torkzaban, S. Colloid interaction energies for physically and chemically heterogeneous porous media. *Langmuir* **2013**, *29* (11), 3668–3676.
- (32) Bedrikovetsky, P.; Siqueira, F. D.; Furtado, C.; de Souza, A. L. S. Modified particle detachment model for colloidal transport in porous media. *J. Transp. Porous Media* **2011**, *86*, 353–383.

- (33) Bedrikovetsky, P.; Zeinijahromi, A.; Siqueira, F. D.; Furtado, C.; de Souza, A. L. S. Particle detachment under velocity alternation during suspension transport in porous media. *J. Transp. Porous Media* **2012**, *v. 91* (1), 173–197.
- (34) Lenhart, J. J.; Saiers, J. E. Colloid mobilization in water-saturated porous media under transient chemical conditions. *Environ. Sci. Technol.* **2003**, *37*, 2780–2787.
- (35) Tosco, T.; Tiraferri, A.; Sethi, R. Ionic strength dependent transport of microparticles in saturated porous media: Modeling mobilization and immobilization phenomena under transient chemical conditions. *Environ. Sci. Technol.* **2009**, *43*, 4425–4431.
- (36) Grolimund, D.; Borkovec, M. Release and transport of colloidal particles in natural porous media: 1. Modeling. *Water Resour. Res.* **2001**, *37*, 559.
- (37) Zhivko, Z.; Rumiana, B.; Hideki, O.; Rajan, J.; Yusuke, I.; Yoshinobu, B. Uncoated, broad fluorescent, and size-homogeneous CdSe quantum dots for bioanalyses. *Anal. Chem.* **2006**, *78*, 321–330.
- (38) Bruchez, M.; Moronne, M.; Gin, P.; Weiss, S.; Alivisatos, A. P. Semiconductor nanocrystals as fluorescent biological labels. *Science* **1998**, *281*, 2013–2016.
- (39) Holttä, P. L.; Lahtinen, M.; Hakanen, M.; Lehto, J.; Juhola, P. Effect of ionic strength on the stability of colloids released from injection grout silica sol. *MRS Proceedings* **2010**, *1265*, 1265-AA06–10, DOI: 10.1557/PROC-1265-AA06-10.
- (40) Bradford, S. A.; Torkzaban, S.; Wiegmann, A. Pore scale simulations to determine the applied hydrodynamic torque and colloid immobilization. *Vadose Zone J.* **2011**, *10*, 252–261.
- (41) Bradford, S. A.; Torkzaban, S.; Shapiro, A. A theoretical analysis of colloid attachment and straining in chemically heterogeneous porous media. *Langmuir* **2013**, *29* (23), 6944–6952.
- (42) Massoudieh, A.; Ginn, T. R. Modeling colloid facilitated transport of multi-species contaminants in unsaturated porous media. *J. Contam. Hydrol.* **2007**, *92* (3), 162–183.
- (43) Nelder, J. A.; Mead, R. A. simplex-method for function minimization. *Comput. J.* **1965**, *7* (4), 308–13.
- (44) Massoudieh, A.; Mathew, A.; Ginn, T. R. Column and batch reactive transport experiment parameter estimation using genetic algorithms. *Comput. Geosci.* **2008a**, *34*, 24–34.
- (45) Massoudieh, A.; Abrishamchi, A.; Kayhanian, M. Mathematical modeling of first flush in highway storm runoff using genetic algorithm. *Sci. Total Environ.* **2008b**, *398* (1–3), 107–121.
- (46) Bergendahl, J.; Grasso, D. Prediction of colloid detachment in a model porous media: Thermodynamics. *AIChE J.* **1999**, *45*, 475–484.
- (47) Kjellander, R.; Marcelja, S.; Pashley, R. M.; Quirk, J. P. Double-layer ion correlation forces restrict calcium clay swelling. *J. Phys. Chem.* **1988**, *92*, 6489–6492.
- (48) Quirk, J. P. Interparticle forces: A basis for the interpretation of soil physical behavior. *Adv. Agron.* **1994**, *53*, 121–183.
- (49) Yuan, H.; Shapiro, A. A. A mathematical model for non-monotonic deposition profiles in deep bed filtration systems. *Chem. Eng. J.* **2011**, *166*, 105–115.
- (50) Alperovitch, N.; Shainberg, I.; Keren, R.; Singer, M. J. Effect of clay mineralogy and Al and Fe oxides on the hydraulic conductivity of clay-sand mixtures. *Clays Clay Miner.* **1985**, *33*, 443–450.
- (51) Sposito, G. *The Chemistry of Soils*, 2nd ed; Oxford University Press: New York, 2008.
- (52) Ryan, J. N.; Gschwend, P. M. Effects of ionic-strength and flow rate on colloid release: Relating kinetics to intersurface potential-energy. *J. Colloid Interface Sci.* **1994**, *164*, 21–34.
- (53) Torkzaban, S.; Hyunjung, N. K.; Simunek, J.; Bradford, S. A. Hysteresis of colloid retention and release in saturated porous media during transients in solution chemistry. *Environ. Sci. Technol.* **2010**, *44*, 1662–1669.